

# High resolution *Chandra* X-ray imaging of the nucleus of M 33

G. Dubus<sup>1,2</sup>, P. A. Charles<sup>3</sup>, and K. S. Long<sup>4</sup>

<sup>1</sup> Laboratoire Leprince-Ringuet, École Polytechnique, 91128 Palaiseau, France  
e-mail: gd@poly.in2p3.fr

<sup>2</sup> Institut d'Astrophysique de Paris, 98bis boulevard Arago, 75013 Paris, France

<sup>3</sup> Department of Physics and Astronomy, University of Southampton, Southampton SO17 1BJ, UK

<sup>4</sup> Space Telescope Science Institute, 3700 San Martin Dr., Baltimore MD 21218, USA

Received 7 May 2004 / Accepted 4 June 2004

**Abstract.** We show with a short *Chandra* HRC-S exposure that the powerful X-ray source coincident with the nucleus of M 33 is unresolved at the highest spatial resolution available to date (0'4). The source flux is variable, doubling during the 5 ks exposure. The combination of properties exhibited by M 33 X-8 establishes the source as the nearest example of the ultra-luminous X-ray sources that have been uncovered in other nearby galaxies. On short timescales, we set limits of 9% rms variability for pulsations in the 0.01–1000 Hz range.

**Key words.** galaxies: individual: M 33 – galaxies: nuclei – galaxies: Local Group – X-rays: galaxies

## 1. Introduction

The nearby galaxy M 33 ( $d \approx 795$  kpc; van den Bergh 1991) hosts the most luminous steady X-ray source in the Local Group: M 33 X-8 has a 1–10 keV luminosity of  $1.2 \times 10^{39}$  erg s<sup>-1</sup>. The source has been detected at this level ever since the first X-ray observations of M 33 (Long et al. 1981; Markert & Rallis 1983).

*Chandra* observations established that M 33 X-8 is coincident with the optical position of the nucleus to the 0'6 uncertainty of the astrometric solution (Dubus & Rutledge 2002). However, the 1500  $M_{\odot}$  upper limit on the mass of a central black hole placed by the measured velocity dispersion (Gebhardt et al. 2001) and the lack of activity at other wavelengths (Long et al. 2002, and references therein) rule out a low luminosity active galactic nucleus.

Ultra-luminous X-ray sources (ULXs) are defined as point sources having X-ray luminosities in excess of the Eddington limit for a 10  $M_{\odot}$  object ( $10^{39}$  erg s<sup>-1</sup>; Fabbiano & White 2003). ULXs could be due to beamed emission from stellar mass-sized neutron stars (NS)/black holes (BH) or truly isotropic emission from 100–1000  $M_{\odot}$  intermediate mass BHs (King et al. 2001). If M 33 X-8 is a single object, then it is the nearest example of a ULX. The detection of a 106 day ~20% modulation in the X-ray flux from M 33 X-8 in a 5 year span of *ROSAT* data (Dubus et al. 1997) and the resemblance of the spectrum to that of black hole binaries (La Parola et al. 2003) support this picture.

*ROSAT* images show M 33 X-8 to be point-like at 5'' resolution (Schulman & Bregman 1995). But diffuse emission from the compact optical nucleus (3'' wide, see Fig. 3 in

Kormendy & McClure 1993) or contributions from close, faint sources would not have been resolved using any pre-*Chandra* instrument. With its superior angular resolution, *Chandra* has been able to reduce the possibility that ULXs in nearby galaxies are chance superpositions of lower luminosity sources. Unfortunately, in the case of M 33 X-8, the existing *Chandra* observations of M 33 X-8 had the nuclear source either far off-axis or heavily piled-up in ACIS CCD. As a result, the *Chandra* data could not be used to study the radial extent below a few arc seconds.

Here we report a new observation of M 33 X-8 with *Chandra*, an on axis observation obtained with the High Resolution Camera (HRC) on board *Chandra* that fully exploits the spatial resolution of *Chandra* in an attempt to resolve the nuclear source in M 33. The observation, spatial and timing analysis are described in Sects. 2–4. The results are discussed in Sect. 5.

## 2. Observation

M 33 was observed with the *Chandra*/HRC-S instrument (Murray et al. 1998) on July 29, 2003 from 19:53:12 UT for a total exposure time of 5355 s. The HRC is unaffected by pile-up and provides the best achievable spatial resolution (0'4 *FWHM*) to date. We decided to use the HRC-S which has the capability to study the poorly known timing properties of M 33 X-8 at frequencies above 1 Hz. We performed the analysis with CIAO version 3.0.1<sup>1</sup>.

There is only one point source, M 33 X-8, with signal-to-noise greater than 5 in the field-of-view. In the 6 × 8'

<sup>1</sup> <http://asc.harvard.edu/ciao>

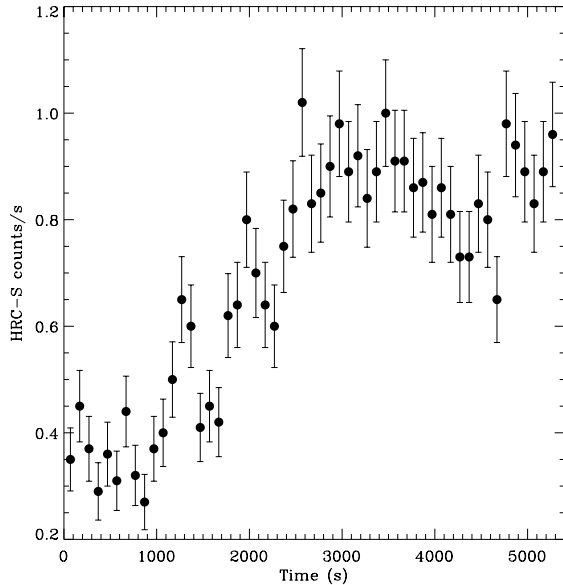


**Fig. 1.** HRC-S lightcurve of M 33 X-8 in 100 s bins, showing significant variability on timescales of  $\sim 1$  ks.

central region surrounding M 33 X-8 where the background is spatially uniform, we estimated the average background rate per  $2''$  circular region, and found that 28 counts would be needed for a  $3\sigma$  detection (taking into account the  $13\,750$  separate trials). This translates into a  $0.6\text{--}9$  keV luminosity upper limit for point source detection in this observation of  $<9 \times 10^{36} (d/795 \text{ kpc})^2 \text{ erg s}^{-1}$  (assuming a photon power-law of  $\alpha = 2$ ,  $N_{\text{H}} = 1.9 \times 10^{21} \text{ cm}^{-2}$ ). There are 43 sources within  $8'$  of M 33 X-8 in the X-ray *ROSAT* catalogue of Haberl & Pietsch (2001) but the brightest of these (excluding X-5 which is at the very edge of the field-of-view) have count rates a factor  $\leq 1\%$  that of M 33 X-8. Hence, it is not surprising that we failed to detect any other sources in this short exposure.

### 3. Timing analysis

We extracted 3756 counts from a 16 pixel radius region around M 33 X-8, giving an average of  $0.70 \pm 0.01 \text{ counts s}^{-1}$ . Using an annulus with inner and outer radii of 20 and 30 pixels, we estimate the background contribution to be only 6 counts (and hence negligible). Surprisingly, the count rate from M 33 X-8 varied significantly during our observation, increasing from  $0.36 \pm 0.03$  to  $0.92 \pm 0.04 \text{ counts s}^{-1}$ , on a timescale of 2400 s (Fig. 1). Previous results have consistently shown that the X-ray spectrum of M 33 X-8 is well fitted by a  $kT = 3.5$  keV thermal bremsstrahlung spectrum with  $N_{\text{H}} = 1.9 \times 10^{21} \text{ cm}^{-2}$  (Takano et al. 1994; Parmar et al. 2001; Dubus & Rutledge 2002; La Parola et al. 2003). Assuming this spectrum (for which 1 HRC-S count corresponds to  $2.6 \times 10^{-11} \text{ erg cm}^{-2}$  of unabsorbed flux in the  $0.6\text{--}9$  keV band), the maximum count rate is equivalent to  $L_{\text{X}} = 1.8 \times 10^{39} (d/795 \text{ kpc})^2 \text{ erg s}^{-1}$ .

We applied barycenter corrections to the photon arrival times and computed their power density spectrum (PDS), with a Nyquist frequency of 1000 Hz. We find no excess power above 0.01 Hz, with a 99.9% upper limit of  $<8.8\%$

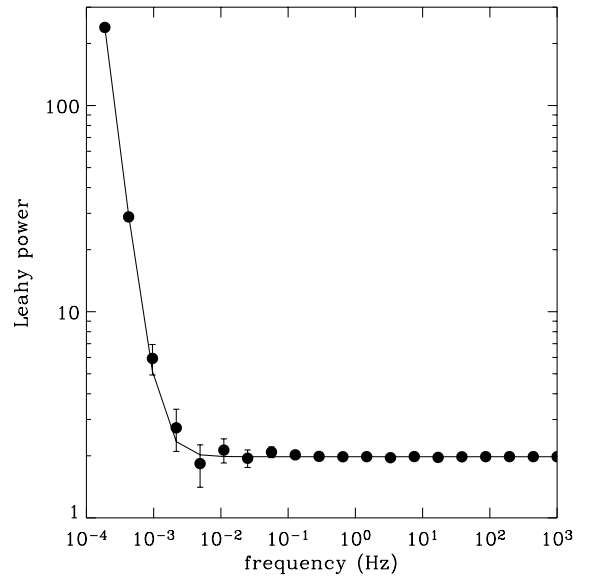


**Fig. 2.** Power Density Spectrum of M 33 X-8 during the 5355 s *Chandra* HRC-S observation, normalized according to Leahy et al. (1983). Data have been rebinned logarithmically. The solid line shows the best-fit power-law (slope  $\alpha = 2.65 \pm 0.15$ ) + constant noise (taken equal to the average at high frequencies, 1.98).

root-mean-squared (rms) variability from a sinusoidal signal. Logarithmically rebinning the PDS to 100 bins, we do not find any excess from broad timing features above  $>0.01$  Hz. The 90% upper limit to a quasi-periodic oscillation (QPO) is 24% rms where we have modeled the QPO as a 0.25 Hz *FWHM* gaussian at 6 Hz. There is significant power at low frequencies with a measured  $30 \pm 6\%$  rms variability below 0.01 Hz. Further rebinning to 20 frequency bins (Fig. 2), we find that the data are well described ( $\chi^2_{\nu} = 0.7$ , 18 degrees of freedom) by a fit to a constant plus a power-law low frequency noise (LFN) with a steep slope  $\alpha = 2.65 \pm 0.15$  (90% confidence error). The constant is taken equal to the high frequency average, 1.98 (close to the expected level from a pure Poisson flux). However, the LFN power must turn over between 0.02 and 0.19 mHz in order for it not to diverge (i.e. exceed 100%). To constrain any additional high frequency, flatter timing feature, we fixed the power-law slope at  $-2.65$  and added a second component with  $\alpha = 1$ . The 90% confidence upper limit to the rms variability below 10 Hz is  $<3.2\%$ , corresponding to a change in the minimum  $\chi^2$  of 4.61 (Lampton et al. 1976).

In spite of the lack of photon energy sensitivity in the HRC detectors, we can still search for spectral variability by exploiting the fact that the photon energy to pulse-invariant (PI) energy channel calibration is stable during an observation. We therefore investigated the data in two ways: firstly by comparing counts in the first 2000 s interval (cf. Fig. 1) with those detected afterwards (a total of 907 and 2829 counts respectively); secondly by dividing in time so as to produce an equal number of counts in each group (which occurs 3172 s into the observation). The distributions of the PI channels between groups are statistically identical (respectively a probability of 0.30 and 0.19 of being drawn from the same distribution for a two-sided Kolmogorov-Smirnov test). Hence, within the

constraints of the HRC, there is no evidence for spectral variability during our observation.

#### 4. Spatial analysis

Our main purpose in undertaking this observation was to determine whether the nuclear source in M 33 is point-like. We therefore used *ChaRT* and *Marx* to simulate how the PSF of M 33 X-8 would appear on the HRC-S detector if it were point-like. In carrying out this simulation (of 28 861 counts in total), we assumed the same spectrum as in Sect. 3. This simulation accounts for all known telescope and detector effects. It also shows why the spectrum is important, as the *ChaRT* PSF is significantly broader than a monochromatic PSF (at 1 keV) calculated with *mkpsf*.

We logarithmically re-binned the data into a 1-D radial distribution (between  $r = 0$  and  $40''$ ) for comparison with a *ChaRT* simulation (Fig. 3). We determined the source centre by rebinning the PSF and performing a radial fit to the data, minimising  $\chi^2$  against the 2-D offset. The best-fit to the PSF model has  $\chi^2_\nu = 1.72$  (18 degrees of freedom), and the simulated PSF is a good description of the data. We find no evidence for any additional component to the emission profile.

Extended emission associated with the nucleus is not statistically required by the data. To place an upper limit on its contribution, we convolved the PSF with the radial profile derived from *Hubble Space Telescope* visible data (Dubus et al. 1999). The 90% confidence upper limit is  $<3.7\%$  of the average flux from M 33 X-8 during the observation or  $4.7 \times 10^{37}$  erg s $^{-1}$ .

We also examined the residuals obtained by subtracting the best-fit PSF from the data using an image bin size of 3 pixels ( $0''.4$ ), equal to the resolution of the HRC-S. There is no apparent structure in the residuals, which have amplitudes smaller than  $<7\%$  of the peak flux. We derive an upper limit of  $9.1 \times 10^{37}$  erg s $^{-1}$  to the contribution from a point source between  $0''.4$ – $1''$  from the nucleus.

#### 5. Discussion

Dubus & Rutledge (2002) established to a high degree of precision that M 33 X-8 is coincident with the nucleus. The present *Chandra* HRC-S observation shows that M 33 X-8 is also unresolved at  $0''.4$  resolution, improving on earlier *ROSAT* HRI upper limits by a factor  $\sim 10$  (Schulman & Bregman 1995). This rules out contributions from nearby sources but does not rule out multiple sources within the compact nucleus core (Dubus et al. 1999). However, the substantial (50%) variability we observe during this short 5 ks observation shows that a single source dominates. We conclude M 33 X-8 is most likely a single source and, as has been claimed previously, the nearest example of a ULX source.

A possible key to uncovering the nature of this source is its variability. The short timescale doubling that we observe is unprecedented: within single pointed observations M 33 X-8 is usually seen to be constant. Variability at a level of 10% has been observed within hours to days in only two *ROSAT* visits (Dubus et al. 1997). More recently, 10% variability on a timescale of 5000 s was seen in a continuous 93 ks *Chandra*

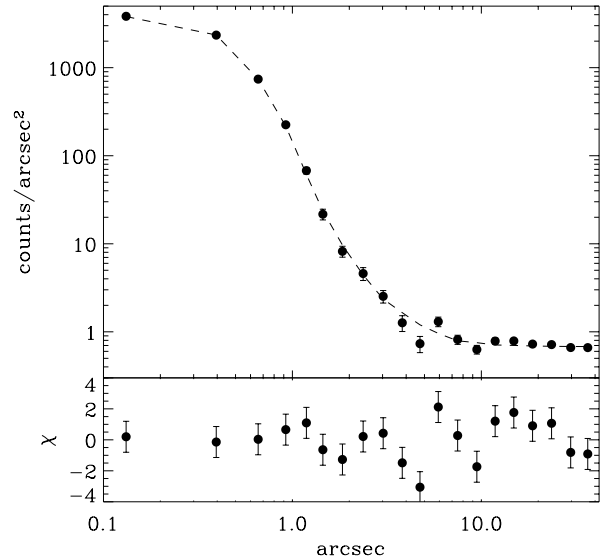


**Fig. 3.** *Top panel:* the observed radial profile of M 33 X-8, showing the number of counts (with Gaussian errors) per unit area in annular bins. The dashed line is the best fit model (from *ChaRT*), and includes a constant background component. M 33 X-8 dominates at radii  $<4''$ , while the background dominates at larger radii. *Bottom panel:* the  $\chi = (\text{data-model})/\sigma$  residuals. We attribute the scatter between radii of 5 and  $40''$  as due to unresolved point sources.

off-axis observation (La Parola et al. 2003; see also Peres et al. 1989 for an earlier report). Although the timescale of the variation we observe is similar, the amplitude in our observation is much larger than the 10% variation observed by La Parola et al. (2003).

Using the doubling timescale of 2400 s, we can set an upper limit to the emission region of  $7 \times 10^{13}$  cm which hints at a compact object. Recently, it has been proposed that the break frequency at which the PDS of active galactic nuclei and X-ray binaries switch from a  $-2$  to a  $-1$  power-law slope depends on the black hole mass (McHardy et al. 2004). Using the fact that the PDS of M 33 X-8 must turn over between 0.02 and 0.19 mHz, and interpreting this break as the high frequency turnover (e.g. NGC 4051, McHardy et al. 2004), we find the black hole mass would be in the range  $10^{5-6} M_\odot$ . This is inconsistent with velocity dispersion upper limits (Gebhardt et al. 2001). Hence, it is unlikely the variability is associated with the high frequency noise phenomenon described by McHardy et al. (2004). Much longer exposures are needed to establish the timing properties of M 33 X-8 and investigate its nature.

The X-ray spectrum, long timescale variability and lack of an optical counterpart suggest an X-ray binary. The  $\sim 1$  h doubling, but lack of fast variability, are consistent with a low mass X-ray binary in the high or very high state. On long timescales, Markert & Rallis (1983) observed a 50% count rate drop between two *Einstein* HRI observations separated by six months. Later *ROSAT* observations confirmed variations of  $\geq 20\%$  on a timescale of 106 days (Dubus et al. 1997). La Parola et al. (2003) have emphasized the similarity between M 33 X-8 and LMC X-3. LMC X-3 has long term variations on a 99 day (or 199 day) timescale (Wilms et al. 2001). We note that the

present observation would correspond to phase  $\phi = 0.87$  in Fig. 3 of Dubus et al. (1997), very close to the minimum of the cycle where the folded *ROSAT* data shows the most scatter.

*Chandra* results indicate that ULXs are more frequently found in association with recent star formation (Fabbiano & White 2003). There is evidence for a 40 Myr old starburst in the nucleus of M 33 (O’Connell 1983; Long et al. 2002). The presence of M 33 X-8 could be linked to this episode of star formation, suggesting perhaps a source comprised of a high mass companion orbiting a stellar-mass black hole. At present, the source in the nucleus of M 33 appears to have all of the characteristics of a canonical ULX. As such, a better understanding of the nearest ULX should remain a priority.

*Acknowledgements.* Support for this work was provided by NASA through *Chandra* Award Number NAS8-39073 issued by the *Chandra* X-ray Observatory Center, which is operated by the Smithsonian Astrophysical Observatory for and on behalf of NASA under contract NAS8-39073.

## References

- Dubus, G., & Rutledge, R. E. 2002, *MNRAS*, 336, 901  
 Dubus, G., Long, K. S., & Charles, P. A. 1999, *ApJ*, 519, L135  
 Dubus, G., Charles, P. A., Long, K. S., & Hakala, P. J. 1997, *ApJ*, 490, L47  
 Fabbiano, G., & White, N. E. 2003, in *Compact Stellar X-ray Sources*, ed. W. H. G. Lewin, & M. van der Klis (Cambridge University Press), in press [arXiv:astro-ph/0307077]  
 Gebhardt, K., Lauer, T. R., Kormendy, J., et al. 2001, *AJ*, 122, 2469  
 Haberl, F., & Pietsch, W. 2001, *A&A*, 373, 438  
 King, A. R., Davies, M. B., Ward, M. J., Fabbiano, G., & Elvis, M. 2001, *ApJ*, 552, L109  
 Kormendy, J., & McClure, R. D. 1993, *AJ*, 105, 1793  
 La Parola, V., Damiani, F., Fabbiano, G., & Peres, G. 2003, *ApJ*, 583, 758  
 Lampton, M., Margon, B., & Bowyer, S. 1976, *ApJ*, 208, 177  
 Leahy, D. A., Darbro, W., Elsner, R. F., et al. 1983, *ApJ*, 266, 160  
 Long, K. S., Charles, P. A., & Dubus, G. 2002, *ApJ*, 569, 204  
 Long, K. S., D’Odorico, S., Charles, P. A., & Dopita, M. A. 1981, *ApJ*, 246, L61  
 Markert, T. H., & Rallis, A. D. 1983, *ApJ*, 275, 571  
 McHardy, I. M., Papadakis, I. E., Uttley, P., Page, M. J., & Mason, K. O. 2004, *MNRAS*, 348, 783  
 Murray, S. S., Chappell, J. H., Kenter, A. T., et al. 1998, *Proc. SPIE*, 3356, 974  
 O’Connell, R. W. 1983, *ApJ*, 267, 80  
 Parmar, A. N., Sidoli, L., Oosterbroek, T., et al. 2001, *A&A*, 368, 420  
 Peres, G., Reale, F., Collura, A., & Fabbiano, G. 1989, *ApJ*, 336, 140  
 Schulman, E., & Bregman, J. N. 1995, *ApJ*, 441, 568  
 Takano, M., Mitsuda, K., Fukazawa, Y., & Nagase, F. 1994, *ApJ*, 436, L47  
 van den Bergh, S. 1991, *PASP*, 103, 609  
 Wilms, J., Nowak, M. A., Pottschmidt, K., et al. 2001, *MNRAS*, 320, 327